**Abstract:** Q-switched microchip laser emitting radiation at wavelength 1338 nm was designed and constructed. This laser was based on a monolith crystal which combines in one piece a cooling undoped part (undoped YAG crystal), an active laser part ($Nd^{3+}$:YAG), and a saturable absorber ($V^{3+}$:YAG, $T_0 = 85\,\%$). The microchip resonator consists of dielectric mirrors directly deposited on the monolith surfaces. The output coupler with reflection 90 % was placed on the $V^{3+}$-doped part. Q-switched microchip laser was tested under pulsed, and CW diode pumping. The pulse length was the same for all regimes and it equals to 6.2 ns. The wavelength of linearly polarized laser emission was 1338 nm. For pulsed pumping the output pulse energy was stable up to mean pump power 1 W and it was equal to 131 $\mu$J, which corresponds to peak power 21 kW. In CW regime for pumping up to 14 W the pulse energy was 37 $\mu$J.

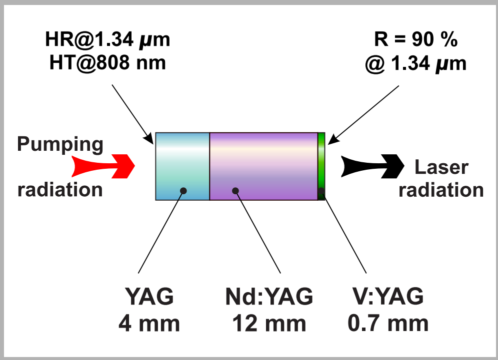


Nd:YAG/V:YAG monolith crystal used Q-switched microchip laser emitting radiation at wavelength 1338 nm.



# Nd:YAG/V:YAG microchip laser operating at 1338 nm

*J. Šulc,* [1,*] *H. Jelínková,* [1] *K. Nejezchleb,* [2] *V. Škoda* [2]

[1] Faculty of Nuclear Sciences and Physical Engineering, Czech Technical University, Prague, Czech Republic
[2] Crytur, Ltd. Turnov, Czech Republic

Received: 2 September 2005, Revised: 4 September 2005, Accepted: 5 September 2005
Published online: 1 January 2006

**Key words:** Nd:YAG, V:YAG, microchip laser, Q-switching

**PACS:** 42.55.Xi, 42.60.Gd

## 1. Introduction

Miniature high peak power laser systems based on microchip geometry[1] are promising radiation sources for many applications, like micromanufacturing, remote sensing, data storage, etc.[2]

In the simplest case, microchip or microcavity laser consists of diode pumped solid state laser passively Q-switched by solid state saturable absorber. For microchip laser construction many different materials were tested but the most experimental work neodymium doped crystals as the gain medium, and $Cr^{4+}$:YAG as the saturable absorber was used.[3]

A specially combination Nd:YAG & Cr:YAG is effective due to e possibility to prepare monolithic composite crystal by direct bonding between the gain crystal, and the saturable absorber.[4] The saturable absorption of $Cr^{4+}$ ions in the near infrared covers spectral range from 0.8 $\mu$m up to 1.2 $\mu$m. From this reason using of the Cr:YAG crystal as the passive Q-switch limits the operating wavelength of the $Nd^{3+}$ ions in the range around 1 $\mu$m, and it is not suitable for longer wavelength transitions, such as 1.3 $\mu$m transitions of $Nd^{3+}$ ions.

As a reliable Q-switch for the 1.3 $\mu$m spectral region, a solid state crystal V:YAG (Yttrium-Aluminum Garnet doped with three-valence vanadium $V^{3+}$) is possible to use, because $V^{3+}$ ions absorbs radiation in the range from 0.9 to 1.5 $\mu$m.[5–7] This saturable absorber was studied in many arrangements together with different $Nd^{3+}$ ions doped hosts.[8–11] The V:YAG crystal was also tested in a microchip geometry for Nd:$YVO_4$ laser Q-switching.[12] The peak power 350 W in 9.3 ns long pulses with repetition rate 8.6 kHz was obtained at the wavelength 1338 nm under 1.5 W pumping.

In this paper we report stable Q-switched output at 1338 nm with length of pulses 6 ns and peak-power 6 kW for CW pumping, and 21 kW for pulsed-pumping obtained from Nd:YAG/V:YAG microchip laser.

* Corresponding author: e-mail: sulc@troja.fjfi.cvut.cz

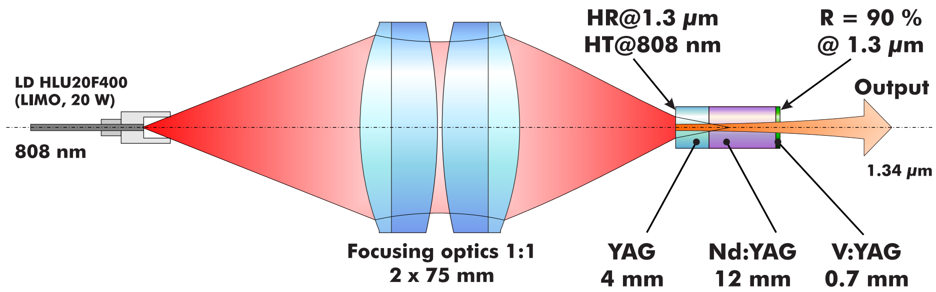


**Figure 1** Longitudinally diode pumped Q-switched laser based on Nd:YAG/V:YAG monolith crystal.

## 2. Materials and methods

The presented in Figure 1 diode pumped Q-switched microchip laser emitting radiation at wavelength 1338 nm was based on a monolith crystal which combines in one piece a cooling undoped YAG part, an active Nd:YAG part, a V:YAG saturable absorber, and laser resonator. The detailed description of particular laser system components is summarized in following subsections.

### *2.1. Nd:YAG/V:YAG microchip crystal*

For a construction of a longitudinally diode pumped Q-switched Nd:YAG laser operating at wavelength 1338 nm a specially developed sandwich crystal was used. This crystal combined in one piece the cooling undoped part (undoped YAG crystal 4 mm long), the active laser part (YAG crystal doped with $Nd^{3+}$ ions, $c = 1.1\,\%$ Nd/Y, 8 mm long), and the saturable absorber (YAG crystal doped with $V^{3+}$ ions 0.7 mm long) – see Figure 2. The diameter of this crystal was 5 mm. Crystal orientation was $<111>$.

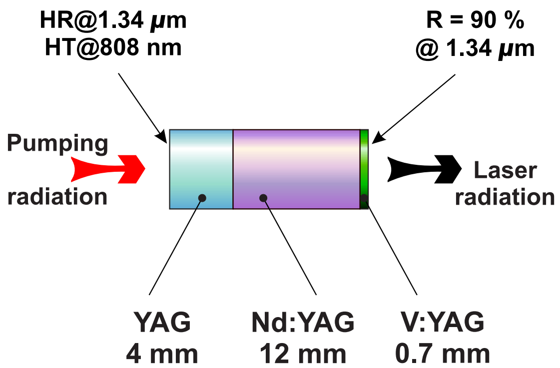


**Figure 2** Layout of Nd:YAG/V:YAG monolith crystal – Q-switched microchip laser emitting radiation at wavelength 1338 nm.

The undoped part was bonded to the pumping face of the crystal $Nd^{3+}$-doped part. It was confirmed[13,14] that using of such undoped part of laser rod enlarges the active material cooling surface and improves the laser active media thermal field uniformity and heatsink.

The V:YAG saturable absorber was diffusion bonded to the un-pumped face of the Nd:YAG section. Thanks to this configuration the effective heat removal from the saturable absorber is accomplished, number of reflecting surfaces and total resonator length was reduced. The initial transmission of the 0.7 mm long V:YAG part was approximately $T_0 \doteq 85\,\%$. This value was set up on the base of previous experiment results to be sure, that the system will reach the lasing threshold.[15]

The microchip resonator consists of dielectric mirrors which were deposited directly on the monolith crystal surfaces. The pump mirror with the high transmission for pump radiation and the high reflection for generated radiation was placed on the undoped YAG part. The output coupler (OC) with reflection 90% for the generated wavelength was placed on the $V^{3+}$-doped part. The total microchip laser resonator length was 16.7 mm. In Figure 3 is presented a photograph of a monolithic composite Nd:YAG/V:YAG Q-switch/amplifying medium device after final polishing and coating.


**Figure 3** Photograph of the monolithic Nd:YAG/V:YAG system prepared by optical contacting followed by diffusion bonding at elevated temperatures.

During the experiment, the microchip crystal was fixed in a water-cooled cupreous heatsink mounted on XYZ-translation stage. Non-stabilized temperature of cooling water was in range from 12 up to 14 °C.

## *2.2. Pumping laser diode & optics*

The pumping source used was a laser diode HLU20F400 (LIMO Laser Systems) emitting radiation at wavelength 808 nm with the maximum output power 20 W at the end of the fiber (fiber core diameter: 400 $\mu$m; numerical aperture: 0.22). The diode radiation was focused into the active Nd:YAG crystal by two achromatic doublet lenses (Thorlabs, Inc., AC508-075-B) with the focal length $f = 75$ mm – see Figure 1. The measured diameter of pumping beam focus was 360 $\mu$m. The pumping beam waist was $\sim 4$ mm long. The active part of the laser crystal absorbed more than 97 % of pumping radiation.

## *2.3. Measuring instruments*

The time characteristics of microlaser output were measured by a fast vacuum photodiode (model FNSPE) with a bias voltage 1000 V. The bandwidth of this photodiode was better than 2 GHz. For a single pulse energy measurement the *Molectron* probe J25 (voltage responsivity 8.59 V/J) was used. With this photodiode and energy probe *Tektronix* oscilloscope TDS 3052B (500 MHz, 5 GS/s) was used. The output mean power was measured by *Molectron* energy/power meter EMP 2000 with the *PowerMax* probe PM3. The spectrum of the laser radiation was investigated by *Oriel* monochromator 77250 (50 $\mu$m wide slit) and it was recorded by the *Electrim* CCD camera EDC-1000HR. Although this camera is based on silicon CCD chip, it is enough sensitive to detect radiation in 1.3 $\mu$m spectral range. The same CCD camera was used for laser beam spatial structure investigation.

## 3. Results and discussion

Constructed Q-switched microchip laser was tested under pulsed (quasi-continuous, QCW), as well as continuous (CW) pumping. Laser radiation parameters – wavelength, polarization, laser beam profile, pulse length, pulse energy or output mean power, and pulse repetition rate – were measured.

## *3.1. QCW Nd:YAG/V:YAG microchip laser*

The Nd:YAG/V:YAG microchip laser was tested under pulsed pumping. The laser diode operates with maximum pump current 30 Amps. The pumping pulse parameters were following: pulse length 250 $\mu$s, maximum power 20 W, and single pulse energy 5 mJ. Adjusting the pulse repetition rate from 2 to 1000 Hz, mean pumping power was controlled in range from 10 mW to 5 W.

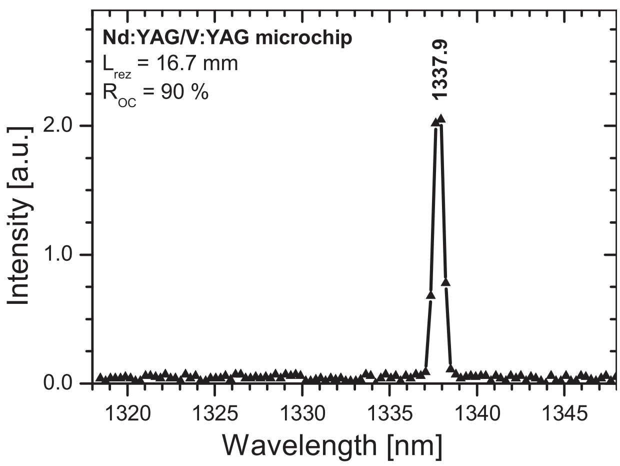


**Figure 4** Emission spectra of Nd:YAG/V:YAG microchip laser under QCW pumping (pulse repetition rate 20 Hz).

### 3.1.1. Laser emission wavelength

Two main emission lines correspond with transition $^4F_{3/2} \rightarrow {}^4I_{13/2}$ of $Nd^{3+}$ ion in YAG.[16] It is stronger emission at wavelength 1318.4 nm, and weaker emission at 1338.2 nm. It was found, that Nd:YAG/V:YAG microchip laser emission corresponds with the second, weaker, transition – measured value was $1337.9$ nm – see Figure 4. Observed line-width $\Delta\lambda \approx 0.4$ nm was on a resolution limit of used method. The emission at this wavelength can be explained by effect of the V:YAG absorption, because its maximum at 1320 nm is closer to Nd:YAG emission at 1318.4 nm. V:YAG absorption at wavelength 1338.2 nm is lower and lasing at this wavelength has lower threshold. It is possible, that for proper shape of OC reflectivity curve, the emission at wavelength 1318.4 nm could reached.

### 3.1.2. Laser emission polarization

Even though all the microchip parts were made from isotropic YAG and pumping radiation was not polarized, we have observed linearly polarized laser emission from examined Nd:YAG/V:YAG microchip laser. Similar effect was observed when Cr:Nd:YAG monolith crystal was operating at 1064 nm.[17] Possible explanation of this effect is a saturation anisotropy in YAG induced by $V^{3+}$-doping. Also, in case of single transversal and longitudinal mode generation, the emission should be linearly polarized.[3] However, single longitudinal mode emission from the Nd:YAG/V:YAG microchip laser was not confirmed yet.

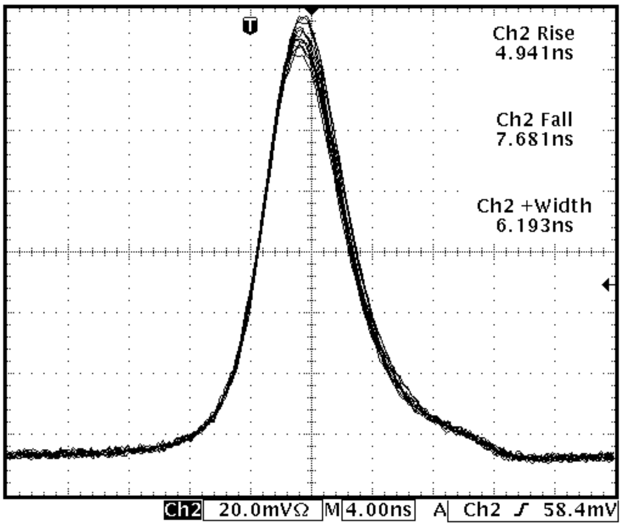


**Figure 5** Time structure of generated radiation of QCW diode-pumped Nd:YAG/V:YAG microchip laser (pulse repetition rate 20 Hz, horizontal resolution 4 ns/div).

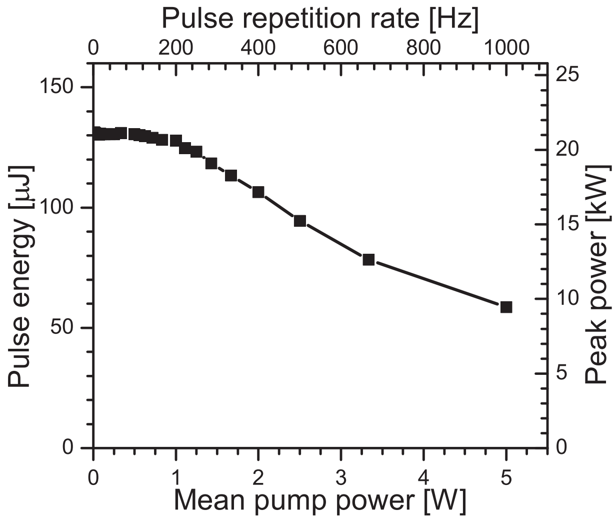


**Figure 6** QCW diode-pumped Nd:YAG/V:YAG microchip laser. Generated pulse energy, and corresponding peak power in dependence on pumping pulse repetition rate or mean power.

### 3.1.3. Laser time & energetic characteristics

In the QCW pumping regime, Nd:YAG/V:YAG microchip laser output pulse energy, and pulse duration were measured and corresponding peak power was calculated. These measurements were done for pulse repetition rates from 2 Hz up to 1 kHz (corresponding mean pumping power from 10 mW to 5 W).

It was found, that the pulse length (FWHM) was equal to $6.2 \pm 0.2$ ns – see Figure 5 – and it did not change with the pumping pulse repetition rate. This well corresponds to the fact that the pulse length is determined mainly by the microchip parameters which are constant.

The generated pulse energy measured directly with the pyroelectric probe did not changed significantly for pumping pulse rep. rate up to 200 Hz and it was equal to $131 \pm 5\ \mu$J. Calculated peak power was 21 kW. For mean pumping power above 1 W, the generated pulse energy was decreasing – see Figure 6. This behaviour can be explained as a thermal lens induced decrease of mode volume inside the gain medium.

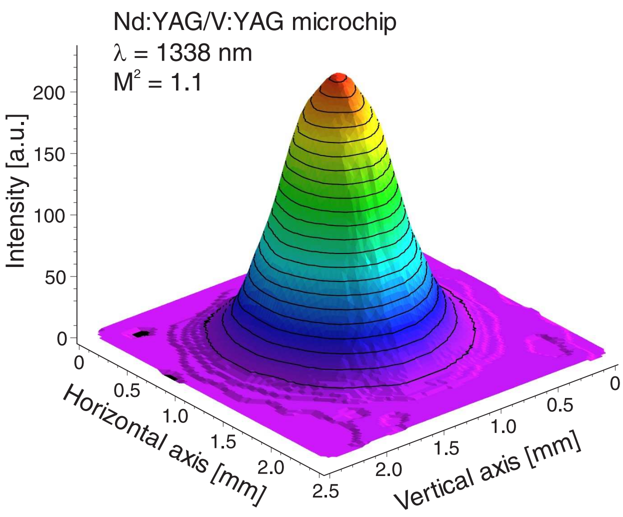


**Figure 7** QCW diode-pumped Nd:YAG/V:YAG microchip laser beam profile measured in distance 300 mm from microchip output (pulse repetition rate 20 Hz).

### 3.1.4. Laser beam spatial structure

Analyzing the space profile of the laser beam for low mean pump power in the QCW regime it was found that the laser beam had a single-mode $TEM_{00}$ nature with the beam parameter $M^2 = 1.1 \pm 0.05$. For mean pumping power 0.1 W the beam profile of laser emission is shown in Figure 7. With increasing mean pumping power the laser beam divergence was slowly increasing. This can be also explained as a thermal lens effect.

## *3.2. CW Nd:YAG/V:YAG microchip laser*

In CW pumping regime, stable repetitive Q-switching was obtained with Nd:YAG/V:YAG microchip laser. Dependence of laser parameters on pumping power was measured. Maximal pumping power used was 14 W. Results are summarized in following subsections.

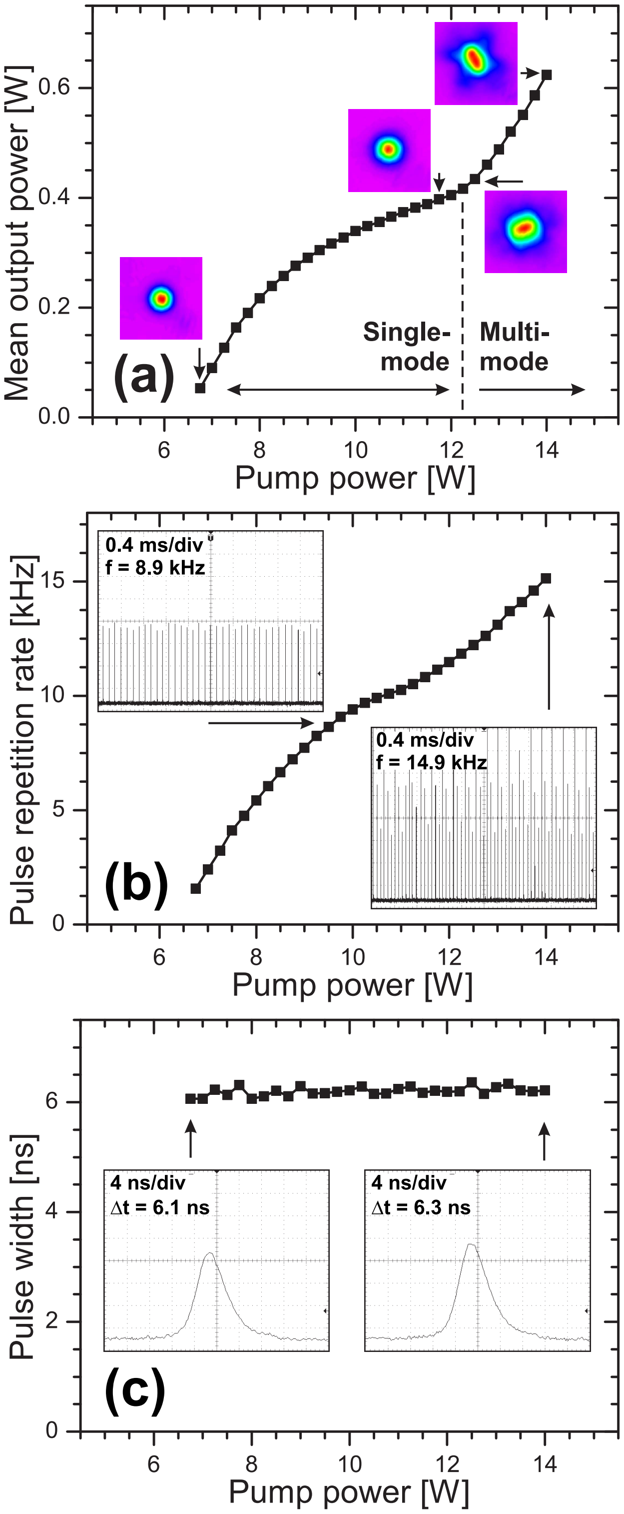


**Figure 8** CW diode-pumped Nd:YAG/V:YAG microchip laser output characteristics: (a) output mean power, (b) pulse repetition rate, and (d) pulse width (FWHM) versus pumping power.

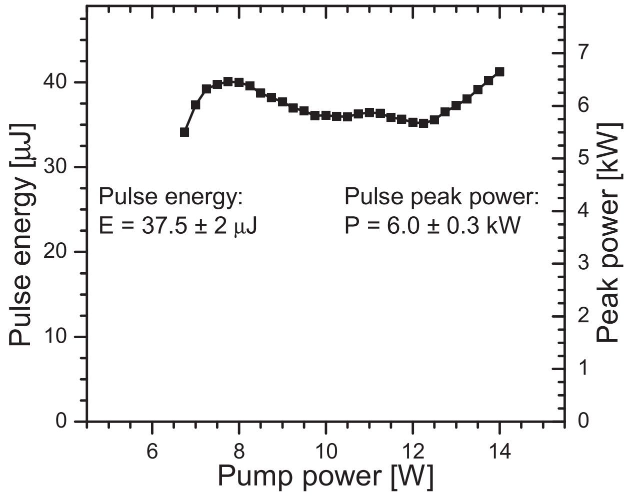


**Figure 9** CW diode-pumped Nd:YAG/V:YAG microchip laser calculated pulse energy and peak power versus pumping power.

### 3.2.1. Laser emission wavelength & polarization

It was found, that CW pumped Nd:YAG/V:YAG microchip laser emission wavelength (1338 nm), and linear radiation polarization, were the same like in case of QCW pumping with lower mean power (see sections 3.1.1 and 3.1.2). These parameters were independent on pumping power.

### 3.2.2. Laser time & energetic characteristics

In dependence on pumping power the Nd:YAG/V:YAG microchip laser output mean power, pulse repetition rate, and pulse width (FWHM) were measured. Results are summarized in Figure 8. The pulse energy was determined from the average output power and pulse repetition rate. The peak power was determined from the pulse energy and average pulse width – see Figure 9.

The Nd:YAG/V:YAG microchip laser threshold pumping power for used pumping system was found to be 6.5 W. With increasing pumping power the mean output power, and generated pulse repetition rate also increased up to 0.6 W and 15 kHz, respectively. The pulse width was independent on pumping power (Figure 8c), and like in the case of QCW pumping, it was equaled to 6.2 ns. The pulse energy and peak power variation with pumping power was $\sim$ 5 % – see Figure 9. Averaged pulse energy and peak power value were $37.5 \pm 2\,\mu$J, and $6 \pm 0.3$ kW, respectively.

The Nd:YAG/V:YAG microchip laser behavior well follows simple concept of CW pumped passively Q-switched laser.[18] The pulse duration is done only by the "second threshold" value affected by the V:YAG saturable absorber initial transmission, OC reflectivity, and resonator length. Because these parameters are in monolithic laser construction perfectly stabilized, the generated pulse width is stable too. Also the pulse repetition rate is well predictable and pulse jitter for constant pumping power is low. Similarly, the pulse energy should be stable and laser output mean power increases only due to increasing pulse repetition rate. But because the pulse energy is also affected by the laser and pump beam volume inside the active medium, some variations due to thermally induced lens was observed – see Figure 9.

#### 3.2.3. Laser beam spatial structure

The Nd:YAG/V:YAG microchip laser beam spatial structure was measured in the whole range of pumping power. Examples of laser beam spatial structure were included in Figure 8a. It was found that for pumping power between laser threshold and 12.5 W, laser was operated in $TEM_{00}$ single-mode regime with beam profile very similar to QCW case plotted in Figure 7. This single-mode generation is favorable affected by presence of saturable absorber which play also role of active aperture preferring low order modes. Due to thermal lens effect, the divergence of the beam was slowly increasing and simultaneously, the beam volume inside the active medium was slowly decreasing, which results in lowering of the output pulses energy.

For pumping power higher than 12.5 W, the laser beam volume inside the active medium was so low in comparison with pumped area, that higher order modes can be generated. This led to pulse energy and mean power increase. As a result of random higher order mode generation, instabilities in pulse peak power could be observed – see Figure 8c, right oscillograph. To suppress these unfavorable effects, better overlapping of pumping beam with single $TEM_{00}$ mode should be used.

## 4. Conclusion

The constructed “alignment-free” Q-switched microchip laser was tested under pulsed (250 $\mu$s long pulses, pump pulse energy 5 mJ), and CW diode pumping. In both cases, the generated pulse energy, pulse length, emission wavelength, polarization, and laser beam profile were measured. It was found, that for all tested regimes the laser has been operating in the single transversal mode $TEM_{00}$ and the generated pulse shape was stable. The pulse length done by the saturable absorber initial transmission, OC reflectivity, and resonator length was equal to $6.2 \pm 0.2$ ns (FWHM) and it was constant for all regimes. The wavelength of linearly polarized laser emission was 1338 nm.

The pulse energy, affected by the laser mode volume in the Nd:YAG part and by microchip construction parameters, depends on the mean pump power. For pulsed pumping the output pulse energy was stable up to mean pump power 1 W (rep. rate 200 Hz) and it was equal to $131 \pm 5\ \mu$J, which corresponds to peak power 21 kW. For mean pump power 5 W (rep. rate 1 kHz), the generated pulse energy drops to 60 $\mu$J due to thermal effects in the laser rod. In CW regime, with the threshold pump power 6.5 W, the pulse energy was approximately stabilized to $37.5 \pm 2\ \mu$J for pumping up to 12.5 W. This energy corresponds to peak power 6 kW. The mean output power increased up to 0.4 W mainly due to increase of the generated pulse repetition rate (11 kHz for mean pump power 12.5 W). For mean pump power higher than 12.5 W, higher order modes were generated and pulse peak power and pulse energy starts to be unstable. In this regime, the maximum mean output power was 0.6 W @ 1338 nm for 14 W pumping power.

## 5. Acknowledgement

Research supported by Czech Ministry of Industry and Trade, project FI-IM2/129 and by Grant of the Czech Ministry of Education MSM 684 0770 022 Laser Systems, radiation and modern optical applications.

## References

[1] J. J. Zayhowski, A. Mooradian, *Opt. Lett.* **14**(1), 24 (1989).
[2] E. Molva, *Opt. Materials* **11**(2–3), 289 (1999).
[3] J. J. Zayhowski, *Opt. Materials* **11**, 255 (1999).
[4] R. Feldman, Y. Shimony, Z. Burshtein, *Opt. Materials* **24**, 393 (2003).
[5] V. P. Mikhailov, N. V. Kuleshov, N. I. Zhavoronkov, P. V. Prokoshin, K. V. Yumashev, *Opt. Materials* **2**(4), 267 (1993).
[6] S. Kück, P. Jander, G. Huber, in *OSA TOPS on Advances Solid State Lasers*, vol. 19 of *Proceedings of OSA*, pp. 509–513 (1998).
[7] Z. Mierczyk, Z. Frukacz, *Opto-Electronics Review* **1**(8), 67 (2000).
[8] H. Jelínková, et al., *Opt. Eng.* **41**(8), 1976 (2002).
[9] A. Agnesi, et al., *Opt. Commun.* **194**(4–6), 429 (2001).
[10] V. P. Mikhailov, et al., in A. A. Pinto, T. Y. Fan (eds.), *Advanced Solid-State lasers*, vol. 15 of *Proceedings of OSA*, pp. 354–358 (1993).
[11] J. K. Jabczyński, et al., *Opt. Eng.* **40**(12), 2802 (2001).
[12] A. M. Malyarevich, et al., *Applied Physics B: Lasers and Optics* **67**(5), 555 (1998).
[13] M. Tsunekane, N. Taguchi, T. Kasamatsu, H. Inaba, *IEEE J. of Selected Topics in Quantum Electron.* **3**(1), 9 (1997), text.
[14] J. Šulc, et al., *Laser Physics, Modern trends in laser physics* **13**(10), 1284 (2003).
[15] J. Šulc, H. Jelínková, M. Němec, K. Nejezchleb, V. Škoda, in A. Sennaroglu, J. G. Fujimoto, C. R. Pollock (eds.), *Solid State Lasers and Amplifiers*, vol. 5460 of *Proceedings of SPIE*, pp. 292–302. SPIE (2004).
[16] W. Koechner, *Solid state laser engeniering*. Springer-Verlag, Berlin, 5th edn. (1999).
[17] S. Li, S. Zhou, P. Wang, Y. C. Chen, *Opt. Lett.* **18**(3), 203 (1993).
[18] A. E. Siegman, *Lasers*. University Science Books, USA (1986).